

Novel Timing Antennas for Improved GNSS Resilience

Erik Lundberg and Ian McMichael

*The Homeland Security Systems Engineering and Development Institute (HSSEDI)TM
Operated by The MITRE Corporation on behalf of the Department of Homeland Security*

BIOGRAPHIES

Dr. Erik Lundberg is a senior signal processing engineer at The MITRE Corporation's National Security Engineering Center. He received a B.S. in physics and a B.A. in mathematics from Augsburg College in 2006, and master's and Ph.D. degrees from Cornell University in electrical and computer engineering in 2011 and 2012. At MITRE, he has worked in the areas of GPS spoofing detection and mitigation; GPS antenna technology; systems engineering; timing; and navigation sensor fusion.

Dr. Ian McMichael received a B.S.E.E. degree from George Mason University in 2001, a M.S.E.E. degree from the George Washington University in 2008, and a Ph.D. degree in electrical and computer engineering from the University of Delaware in 2013. From 2002 to 2013, he was with the U.S. Army Research, Development, and Engineering Command Communications-Electronics Research, Development and Engineering Center (RDECOM CERDEC) Night Vision and Electronic Sensors Directorate, Ft. Belvoir, researching and developing electromagnetic sensors for landmine detection, computational electromagnetics, antenna design, and high impedance ground planes. From 2013 to 2014, he was with Raytheon Integration Defense Systems in Sudbury, Mass., contributing antenna and microwave structure designs. Since 2014, he has been with The MITRE Corporation in Bedford, Mass., contributing to antenna design, radome analysis, and computational electromagnetics.

ABSTRACT

Global Navigation Satellite System (GNSS) antennas installed at fixed site infrastructure are susceptible to interference, jamming, and spoofing signals incident along the direction of the horizon. In this paper, a set of requirements are derived for GNSS antennas that ensure critical infrastructure timing receivers have access to sufficient satellites to derive resilient time and frequency while placing a null in all polarizations at and below the horizon. Multiple quadrifilar helix antennas that meet these requirements are also presented. The efficacy of the designs is demonstrated with field test results. The salient feature of these antennas is a null in the gain pattern in the direction of the horizon and around all azimuth angles to suppress ground-based interference. Other types of antennas have been developed to minimize interference, such as controlled reception pattern antennas. However, none of these antennas simultaneously have sufficient performance, size, weight, power, and cost for widespread applications in commercial and military installations. The proposed high-performance antennas provide GNSS resilience in a small form factor at a low-cost due to the simple architecture.

The first antenna operates at L1 (1.575 GHz) and employs a novel method of reactive loading along the length of the multi-turn helix. The phase distribution along the helix creates a deep null in the gain pattern at the horizon while maintaining sufficient beamwidth in the zenith direction. The prototype antenna is 7.5 inches tall, 1 inch in diameter, and is mounted on a 7-inch diameter ground plane. Gain pattern measurements exhibit a 4.0 dBiC zenith gain and a zenith-to-horizon gain ratio (i.e. null depth) of 29 dB for right hand circular polarization (RHCP) and 34 dB for left hand circular polarization (LHCP). This horizon null minimizes ground based interference. The half power beamwidth (HPBW) of this antenna is approximately 100°, which is sufficient to have access to the required number of satellites for timing applications at least 99 percent of the time.

The second antenna operates at L1 and achieves a horizon null by varying the pitch of the helix arms along the length of the antenna. The variable pitch antenna prototype is 7.8 inches tall, 1.4 inches in diameter, and is mounted on a 7-inch diameter ground plane. Gain pattern measurements exhibit a zenith gain of 7.5 dBiC and a 30-dB zenith-to-horizon ratio for both

RHCP and LHCP. The measured HPBW is 60°, which is sufficient to have access to the required number of satellites for timing at least 95 percent of the time.

INTRODUCTION

Over the last two decades GNSS receivers have been increasingly used to provide time and frequency for synchronization in critical infrastructure. In fact, a 2012 study by the U.S. Department of Homeland Security (DHS) found that 15 of 18 critical infrastructure and key resources sectors relied on the global positioning system (GPS) and GPS receivers for timing [1]. Jamming [2], spoofing [3], and unintentional interference [4] that negatively impacts the reliable, uninterrupted operation of the GPS receiver could potentially threaten these sectors. Spoofing is seen as particularly dangerous since a sophisticated spoofer can control the output of its target GPS receiver without interruption or detection. The demonstration of a successful GPS spoofing attack on a synchrophasor measurement unit in reference [5] illustrates the potential vulnerability of the energy and electric power sub-sector.

The antenna presents a first line of protection for a GPS receiver in the face of over the air radio frequency interference. One common approach, called a controlled reception pattern antenna (CRPA), is to use an array of antenna elements to steer nulls towards detected interference sources and, possibly, beams towards the GPS satellites [6]. This drastically increases the cost, complexity, and power consumption of CRPAs compared to their static gain pattern counterparts. An alternative approach is to design an antenna with a fixed gain pattern with nulls pointed towards the most likely direction of interference. An example of this is multipath mitigation antennas which are designed to have minimal gain in LHCP.

Figure 1 illustrates how a fixed gain pattern antenna could be used to protect GPS timing receivers by attenuating interference originating at, or below, the antenna's horizon. The left-hand side of Figure 1 shows the antenna pattern for a standard GPS timing antenna whose design attempts to place uniform gain over the entire upper hemisphere to maximize the number of satellites visible. This means that the receiver is sensitive to interference coming from the ground. An alternative design is shown in the right-hand side of Figure 1 where the antenna attempts to place a null at and below its horizon. This attenuates all signals, including those from GPS satellites, at low elevations angles. To have the same effect, the ground-based interference source is required to transmit at much higher power.

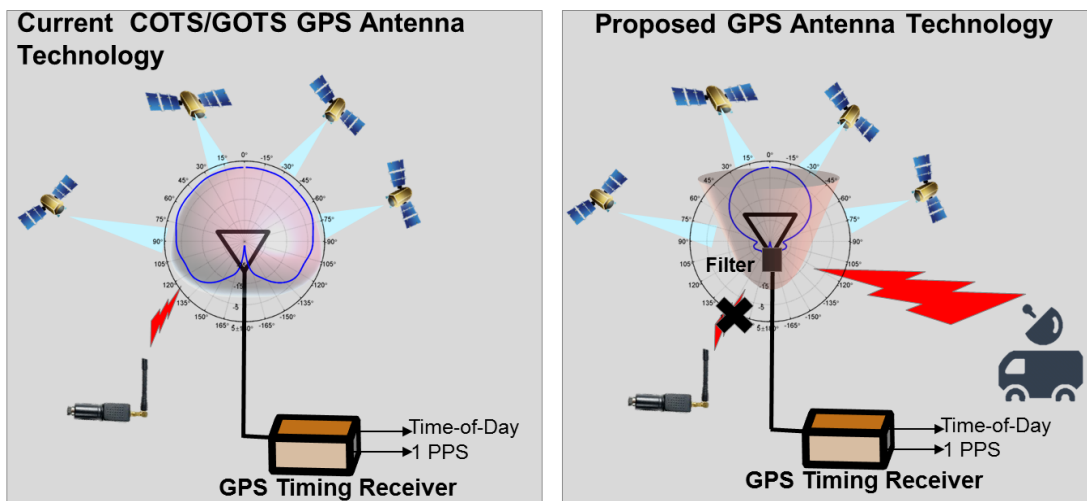


Figure 1. Horizon Nulling Antenna Design Motivation.

A by-product of the horizon null is increased attenuation of the satellite signals at low and moderate elevations (between 0 and about 45 degrees). This trade-off is acceptable because a GPS receiver connected to an antenna with a known location can determine time with adequate precision to critical infrastructure synchronization using a single GPS satellite. To fully reap the benefits of the directional (also known as blocking) antenna, it should be installed in accordance with DHS's recently published best practices [7].

The objectives of this paper are to quantify the minimum beamwidth required to ensure sufficient GPS satellite visibility for timing applications over all landmasses on earth, to present prototype antenna designs that meet and exceed these requirements, and to demonstrate the approach at a field test. Tracking of two satellites is considered sufficient for timing applications since it ensures that satellite faults can be detected [8].

This paper is organized into six additional subsections. First, the results from surveys of GPS antennas and timing receivers are presented. The next two sections describe a global availability simulation environment and results obtained using that environment which inform minimum half power beamwidth requirements. The analysis is followed by a presentation of the prototype antennas whose design was informed by the analysis. The penultimate section presents field test results demonstrating the efficacy of the concept using the prototype antennas. The final section collects important findings and presents conclusions.

ANTENNA AND RECEIVER SURVEY RESULTS

Prior to undertaking the antenna design effort, surveys of available and prototype GNSS antennas and GPS timing receivers were conducted. The antennas are characterized by two figures of merit: the zenith-to-horizon gain ratio and the HPBW. The zenith-to-horizon gain ratio captures the relative interference attenuation and higher is better. The half-power beamwidth is proportional to the satellite visibility. Standard GNSS antenna design seeks to increase HPBW without considering zenith-to-horizon ratio.

Results of the antenna survey are shown in Figure 2 where the y-axis is the right hand circular polarization (RHCP) zenith to horizon ratio and the x-axis is the half-power beamwidth. The narrow beamwidth antennas (HPBW less than 50 degrees) are a highly directional phased array designed for spatial selective transmission, and a horn used in an anechoic antenna measurement chamber. The antennas with a 60-degree HPBW from the prototype horizon ring nuller (HRN) [9]. Multipath mitigation antennas such as choke rings typically have a 100-degree HPBW, and standard timing antennas have a HPBW of greater than 150 degrees. The roughly linear trend between HPBW and zenith-to-horizon ratio makes sense—as the antenna becomes more directional (e.g. smaller HPBW) there is less gain off the main beam.

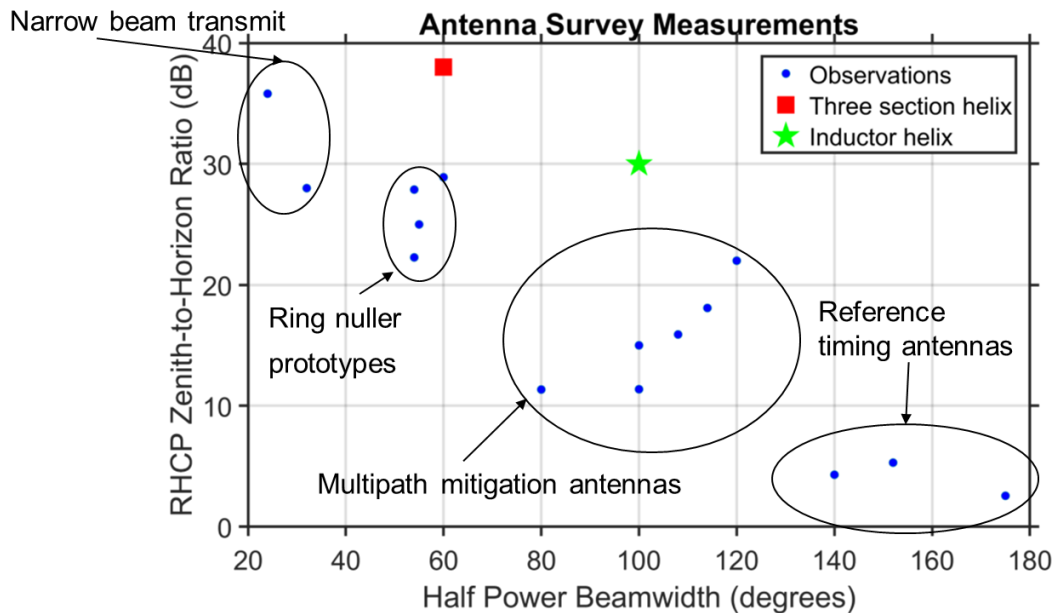


Figure 2. Antenna Survey Results.

The objectives of the GPS receiver survey were to determine whether typical GPS timing antennas implement a “one satellite timing mode” where the receiver can determine time with access to a single GPS satellite signal, and to characterize the receivers’ sensitivity. The intent of the survey was to understand a typical subset of timing receivers and is neither comprehensive nor authoritative. Table 1 shows the results of the survey which revealed that five of the six receivers had a single satellite timing mode.

Receiver sensitivity is quantified by the minimum carrier-to-noise ratio (C/N0) ratio required for acquisition, re-acquisition, and tracking. These thresholds were determined by connecting the receivers under test to a GPS signal simulator. First, the receivers were exposed to sufficient satellites at typical earth coverage power level to determine their position and fully demodulate the 12.5-minute GPS data message. Then the power on a single satellite was decreased until the receiver stopped reporting its tracking state and was recorded as the tracking threshold. The power was then increased until the satellite was again reported by the receiver, which was recorded as the re-acquisition threshold. The acquisition threshold was determined by slowly increasing the power on all signals until the receiver could determine a position fix.

Table 1. Results of the Timing Receiver Survey and Characterization.

Receiver ID	Acquisition (dB-Hz)	Re-Acquisition (dB-Hz)	Tracking (dB-Hz)	1 SV	Industry
Receiver 1	28	N/A	25	Yes	Many
Receiver 2	41	41	36	Yes	Industrial automation and control, cellular communications
Receiver 3	35	N/A	28	Yes	Power grid
Receiver 4	38	37	33	Yes	Precise timing
Receiver 5	44	38	38	No	Cellular communications
Receiver 6	41	36	33	Yes	Cellular communications

Several of the receivers report “signal power” in either unitless decibels or in absolute power (e.g., dBm), which were transformed to C/N0 by engineering judgement. All the measurements in Table 1 are as reported by the receiver and do not reflect the absolute power coming from the simulator. Substantially more testing and quantification is required to fully assess timing receiver sensitivity.

GLOBAL AVAILABILITY SIMULATION

A simulation analysis was performed to determine the minimum antenna beamwidth required to guarantee tracking of at least two GPS satellites for a user on land at least 99 percent of the time.

The general simulation process is shown Figure 3. The goal of the simulation is to calculate the number of satellites visible to each receiver as a function of a given antenna pattern. Each block of the process relies on an important set of parameters. First satellite orbits are calculated. The satellite positions are then used to calculate the C/N0 received at an array of the receiver locations, which depends on the transmit and receive antenna patterns, the transmit power, and the free-space-path-loss. Finally, this array of C/N0 consumed by a GPS receiver model calculates the number of visible satellites for each receiver above which are then statistically analyzed.

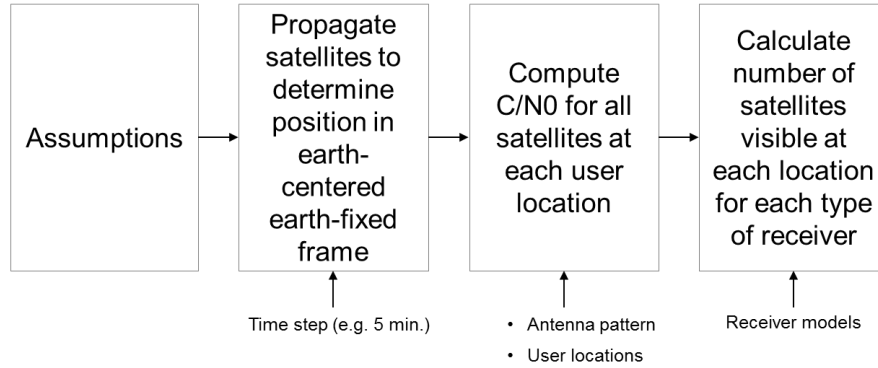


Figure 3. Simulation Processing Flow.

The receive antenna pattern comes from either measured antenna patterns or a simple model. The simple model provides an algorithmic way to determine an antenna pattern for a given HPBW. Real antenna patterns are used to validate the simple model and to predict the prototype antenna performance.

Simulation Link Budget

The carrier power for a single signal from a single satellite at the output of a receive antenna element is given by:

$$P_R = P_{tx} + G_{tx} + L_{path} + G_{rx}$$

Where P_{tx} is the power output by the satellite's power amplifier, G_{tx} is the satellite antenna's gain pattern, L_{path} is the path loss between the satellite and antenna using a simple r^{-2} path loss model, which is a function of the satellite and receiver positions, and G_{rx} is the receive antenna gain in dBi [10].

The minimum and maximum power loss between the satellite antenna and the surface of the earth for satellites above 5 degrees is shown in the bottom of Table 2. Each satellite is assumed to transmit four different signals: coarse acquisition (C/A), precise (P), modernized civilian (L1C), and modernized military (M). The transmit power (P_{tx}) for each of the four signals is given and used to calculate the minimum GPS band power received at the surface of the earth. Since the objective of the simulation is to assess receive antennas, G_{rx} is 0 for the calculations in Table 2.

Only the L1 frequency is simulated and it is assumed that all satellites transmit four different signals: C/A, P, L1C, and M. At each simulated receive antenna, at each simulated time, the noise plus interference is calculated assuming -201.5 dBW/Hz of thermal noise and using spectral separation coefficients (SSC) to account for GPS self-interference [11]. The spectral separation coefficients are calculated assuming a 6 MHz brick-wall receive filter. The spectral separation coefficients are given in Table 2.

Table 2. Spectral Separation Coefficients, P_{tx} , Max. and Min. Received Signal Strength.

Signal	SSC of signal on CA (Hz^{-1})	P_{tx} (dBW)	Min. Power (dBW)	Max. Power (dBW)
C/A	-61.8	12	-158.2	-156.1
P	-70.0	7	-163.2	-161.1
M	-88.9	12	-159.2	-153.0
L1C	-67.9	8.6	-161.6	-159.5
$G_{tx} + L_{path}$	Min	Max		
C/A, P, L1C	-170.2	-168.1		
M	-171.2	-165		

Two different satellite transmit antenna patterns are used, one for CA, P and L1C, and a second for M. The antenna patterns are plotted in Figure 4. The values for the satellite antenna gain are provided in reference [12].

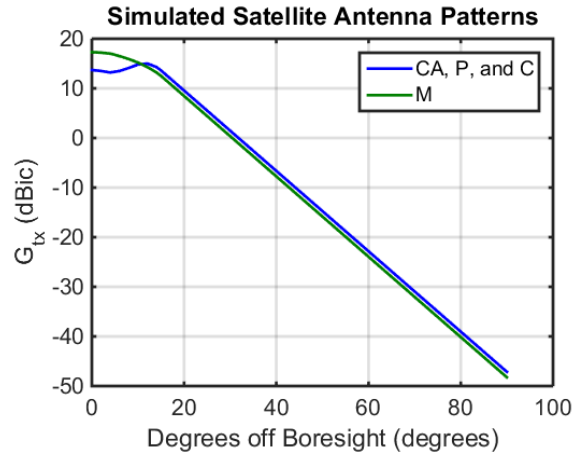


Figure 4. Simulated Transmit Antenna Patterns.

Additional Simulation Details

The satellite positions used in the simulation were calculated using the procedures outlined in IS-GPS-200H [13] and the YUMA almanacs for 09-07-2014 and are provided in Appendix A of reference [12].

Satellite locations were calculated once every five minutes for a single 12-hour GPS orbit.

Modelled Receiver Locations

The primary set of receiver locations used in the simulation are shown in Figure 5 where each dot is at the location of the simulated antenna and receiver. A procedure was developed to distribute the points across all large land masses and islands. The file “landareas.shp” included the mapping toolbox in MatLab 2014B, which encodes the major landmasses on earth in to 537 distinct objects, formed the basis of the procedure. Within each landmass object there may or may not be large bodies of water. First, a set of latitude and longitude points were generated at specified maximum spacing between points. The longitudinal distribution was weighted by latitude to ensure uniform sampling. Each point was tested to see if it was one of the 537 landmasses and to determine whether it was retained or discarded. If the total number of retained points was below a user defined minimum threshold, the maximum spacing was cut in half and the process was repeated. This resulted in a total of 1861 points for a user defined minimum threshold of 1000.

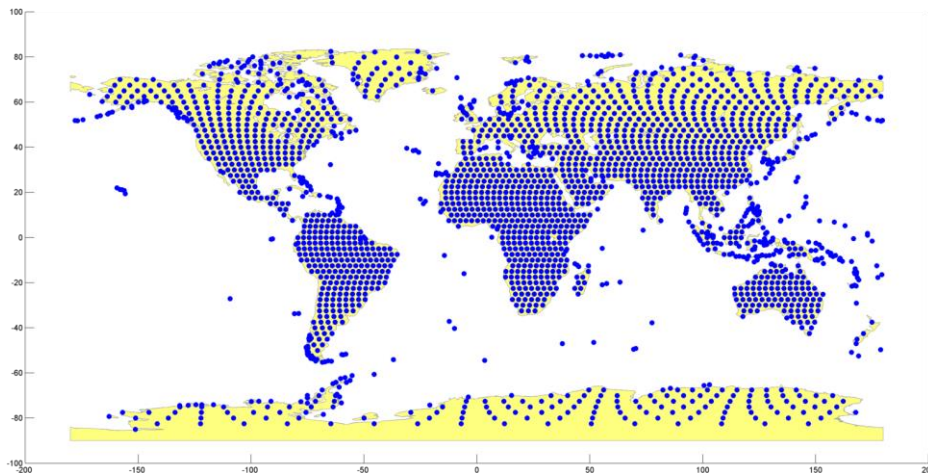


Figure 5. Modelled Receiver Locations.

The analysis focused on all land masses rather than just the United States due to the high degree of international interconnectedness in many critical infrastructure applications. For instance, power grid transmission lines can cross national borders and communication systems span entire oceans.

Raised Cosine Antenna Model

To rigorously analyze the effect of antenna HPBW for GPS timing applications, it is important to have a technique to generate antenna patterns with a given HPBW algorithmically. The following raised cosine antenna model is adapted from reference [14] :

$$G(\theta) = 10 \log_{10} \left(\frac{31000}{HPBW^2} \cos^n \theta \right) \text{ when } \theta \geq .1 \text{ degrees} \tag{1}$$

$$G(\theta) = G(\theta = .1) \text{ when } \theta < .1 \text{ degrees} \tag{2}$$

where θ is an elevation angle in the antenna frame measured in degree from the horizon and $HPBW$ is a user supplied half-power beamwidth in degrees. The power n is a function of $HPBW$:

$$n = \frac{.69}{\log \left(\cos \left(\frac{HPBW}{2} \right) \right)} \tag{3}$$

The raised cosine model described above provides a straightforward way to generate antenna patterns for any given HPBW. Figure 6 shows zenith gain as a function HPBW for the raised cosine model.

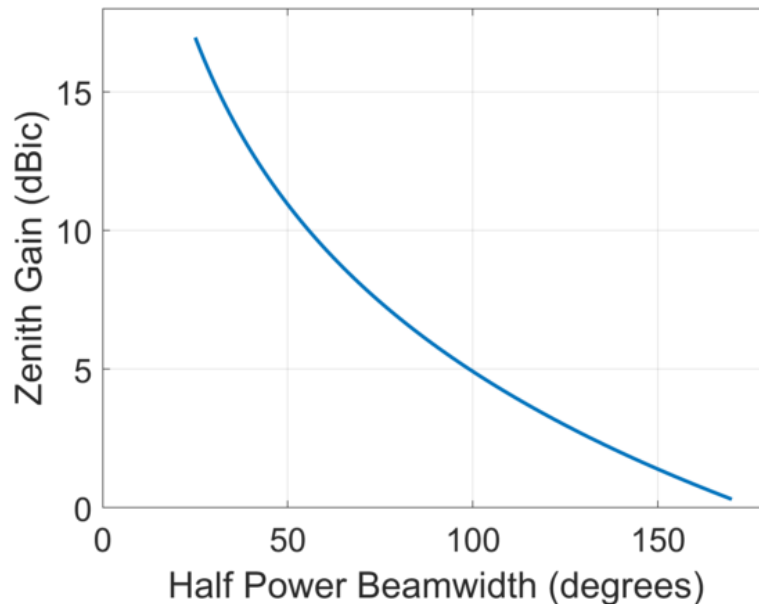


Figure 6. Zenith Gain as a Function of HPBW for Raised Cosine Antenna Model.

Comparison with Measured Patterns

Figure 7 compares the raised cosine antenna model to measured antenna gain patterns for a variety of different HPBW antennas. Each measured antenna pattern was analyzed to find the HPBW of the antenna’s main beam. The measured HPBW was then inserted into raised cosine model. The upper two antennas are directional transmit antennas used for measuring antenna patterns (left) and for high power jamming (right). The lower patterns are example GPS receive antennas. The lower left is from a legacy prototype horizon ring nuller that only nulls RHCP [9]. The lower right is a standard timing antenna.

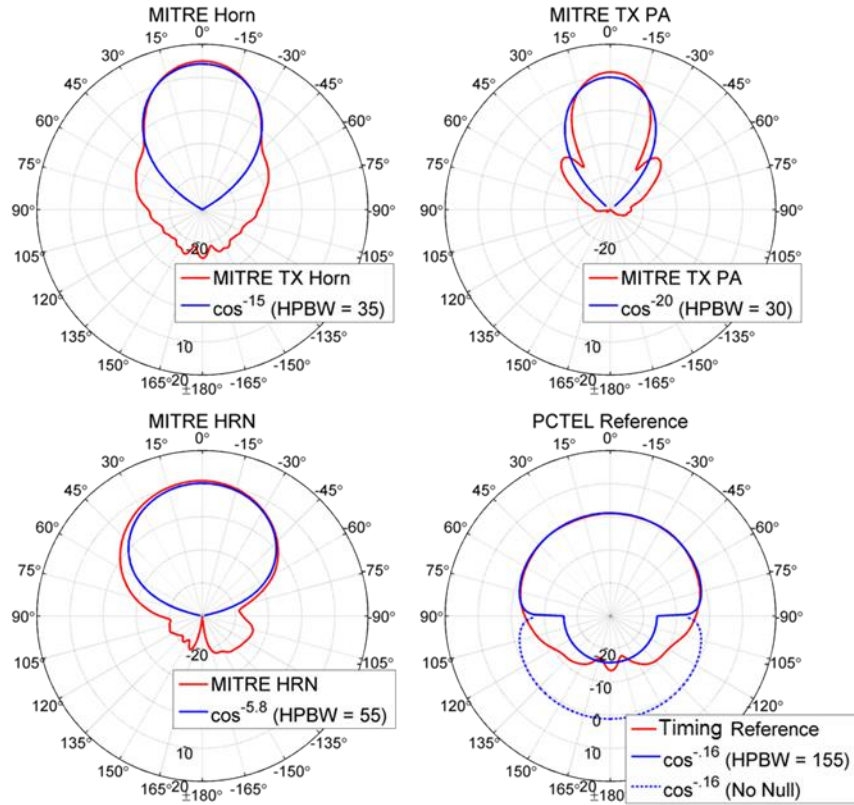


Figure 7. Comparison Between Raised Cosine Model and Measured Gain Patterns for a Variety of Different Antennas.

Within plus or minus 45 degrees of zenith, the raised cosine model never differs from the measured antenna by more than 3 dB with typical differences being less than 1 dB. Since the raised cosine model does not model sidelobes and backlobes, all measured antenna patterns have larger gain at low elevations than the model. In this respect, the model is conservative in that it will underestimate the satellite availability at low elevations.

The top half of Figure 8 repeats the antenna pattern comparison shown above and the bottom half shows satellite visibility probability density functions for various receivers. The bottom plots were generated using the simulation environment that was detailed above. The red traces correspond to the measured pattern and the blue correspond to the raised cosine model. In each of the nine plots, the peak of the red trace occurs to the right of the peak of the blue indicating that the actual antennas are likely to see more satellites than the raised cosine approximation. Therefore, the raised cosine model is conservative.

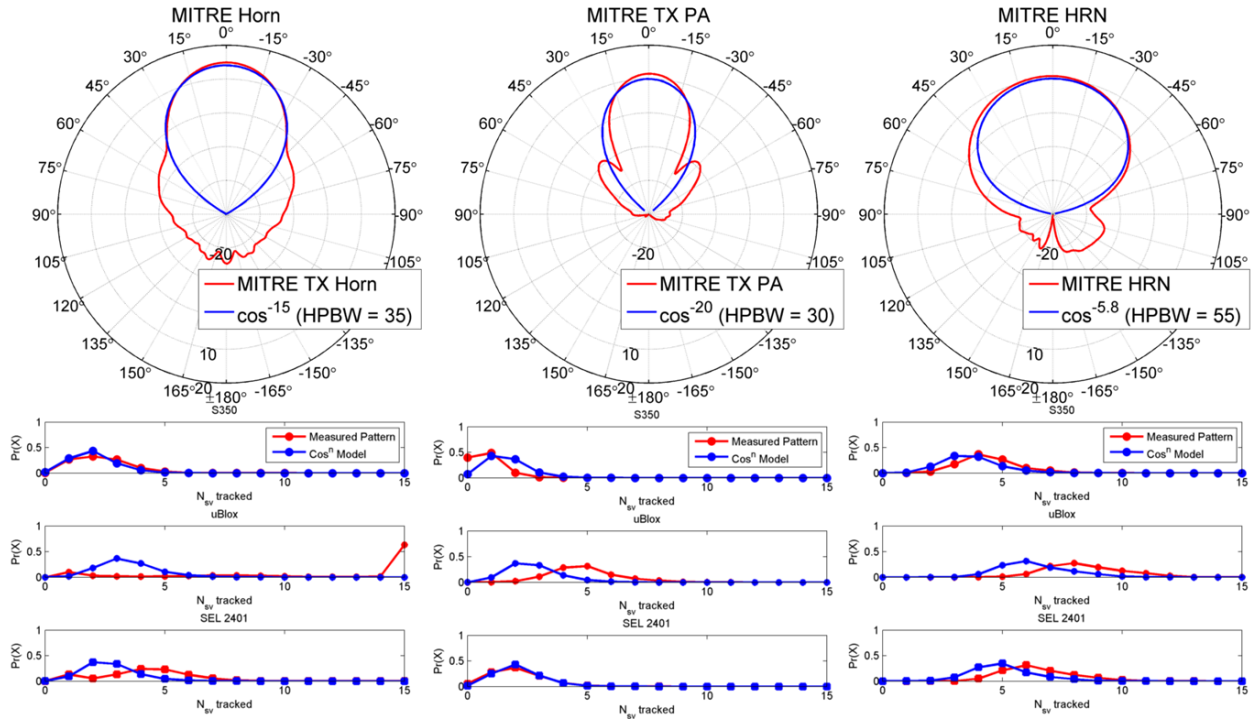


Figure 8. Measured Antenna Patterns Compared to Raised Cosine Model (Top) and Satellite Visibility Probability Density Functions (Bottom).

SIMULATION RESULTS, ANALYSIS, AND DISCUSSION

The simulation described above is used to determine the minimum HPBW for the blocking antenna to provide enough satellite visibility for an appropriately configured GPS receiver to determine time. Inputs to the simulation are the parameters described above, the receive antenna pattern, and the number of locations to be simulated. The output of the simulation is a set of probability distribution functions that quantify the number of satellites tracked over every simulated position for an entire sidereal day for each type of receiver. The simulation output is sensitive to GPS constellation and transmit power, receiver positions, and receiver thresholds, among other parameters.

Quantifying global GPS time availability is difficult because of the vast variability amongst timing receiver sensitivity, different systems' timing requirements, and specific GPS disciplined oscillator implementation and installation details. As described above, receivers with a known antenna location may require only one GPS satellite to be visible to determine time. A receiver that relies on a single satellite to determine time is vulnerable to faults on that satellite since the satellite error will directly map into a time error. Depending on receiver design and algorithm implementation, two satellites are required to detect a fault, and three are required to exclude the fault [8].

Results: Landmass Including Islands and Current GPS Constellation

The baseline simulation scenario uses the receiver locations described above, and the YUMA almanacs described Appendix A of reference [12].

Figure 9 plots the probability that a receiver will see satellites two, three, four or five as a function of antenna HPBW. The vertical arrows identify the beamwidth required to ensure that at least the specified number of satellites are visible over 99 percent of space and time. The 99th percentile threshold is somewhat arbitrary. Lowering the threshold will push the vertical arrows to the left and raising it will push the arrows to the right.

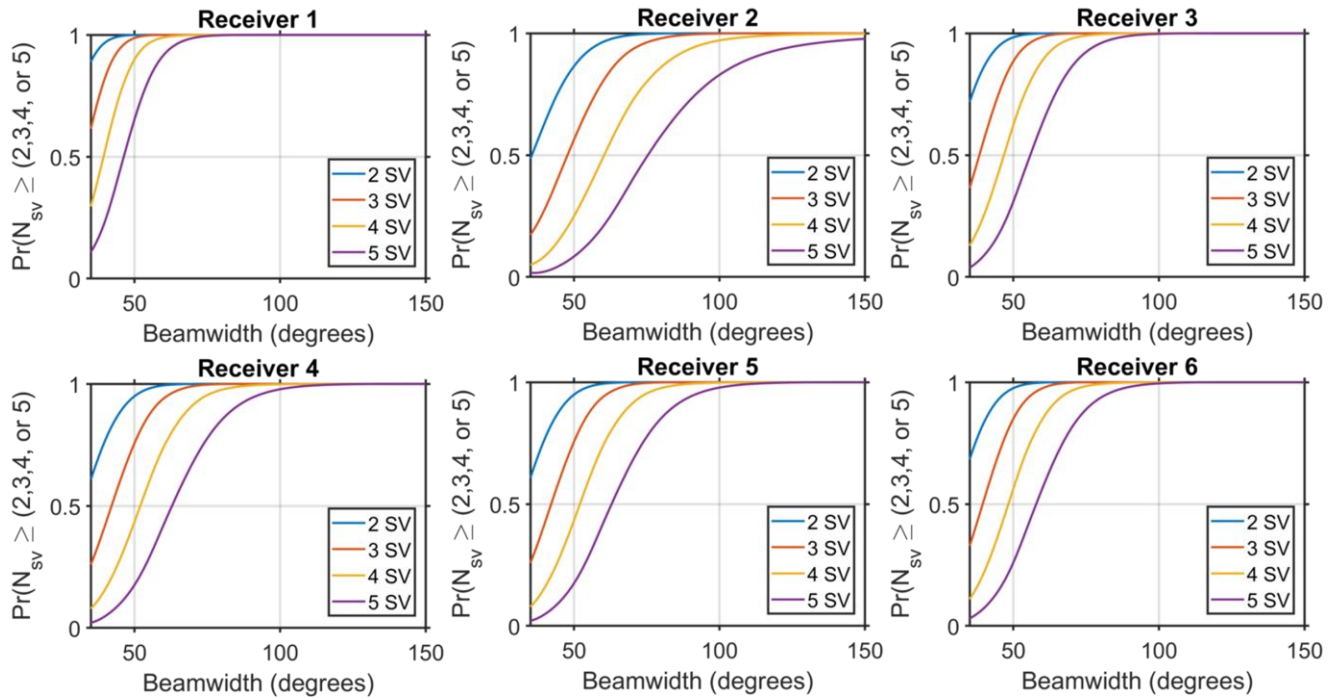


Figure 9. Satellite Visibility as a Function of HPBW for Six Different Receivers.

Figure 9 illustrate the relationship between a receiver’s sensitivity and its ability to provide time. Surprisingly, the least sensitive receiver, receiver three, doesn’t provide global five satellite coverage for a standard timing antenna with a 150-degree HPBW.

Table 3 collects the results plotted in Figure 9. Receiver three’s HPBW thresholds are substantially larger than any of the other receivers. Intuitively, a wider beamwidth antenna will have larger gain at the horizon. Protecting receiver three requires 15 to 30-degree wider beamwidth antennas than any of the other receivers, which equates to 3-6 dB degradation in interference mitigation performance. Receiver three has the highest re-acquisition threshold indicating the sensitivity to this parameter.

Table 3. Beamwidth Required to Ensure 99 percent of the Time Availability for Different Receivers and Satellite Requirements.

Receiver	Number of Satellites			
	2	3	4	5
1	44	51	61	72
2	52	62	75	91
3	68	86	116	-
4	58	69	86	108
5	58	69	86	108
6	54	64	78	95

Preliminary analysis included receivers one, two, and three. For receivers one and two, the three-satellite fault exclusion requirement is met by a 60-degree HPBW antenna. Table 4 shows the satellite availability for a 60-degree HPBW antenna. Three or more SVs are available over 94 percent of space and time for the receivers four and five, and 97.5 percent for receiver six. Per an empirical linear fit to the blue dots in Figure 2, the 70-degree HPBW required for these receivers to reach

the 99 percent threshold will impart a 2-dB degradation in interference suppression. The large gap in measured beamwidths between 60 degrees and 100 degrees decreases the confidence in the empirical fit in this region.

Table 4. Satellite Availability for a 60 Degree HPBW Antenna.

Receiver	Number of Satellites			
	2	3	4	5
1	1	1	0.99	0.92
2	0.999	0.99	0.889	0.632
3	0.965	0.804	0.491	0.21
4	0.994	0.94	0.741	0.42
5	0.994	0.94	0.741	0.42
6	0.999	0.975	0.849	0.566

PROTOTYPE HORIZON NULLING HELIX ANTENNA DESIGNS

Two prototype helix antennas were developed to place a null at all polarizations with a HPBW of at least 60 degrees to meet the requirements described above. These prototype antennas were developed in three stages 1) simulation design, 2) copper tape prototype, and 3) flexible printed circuit prototype. Detailed discussion of the prototype helix antenna electromagnetic design is given in reference [15]. Figure 10 shows the prototype for the three-section helix (TSH) antenna that has a 60-degree HPWB. The important zenith gain, LHCP and RHCP null-depth for the TSH are given in Table 5.

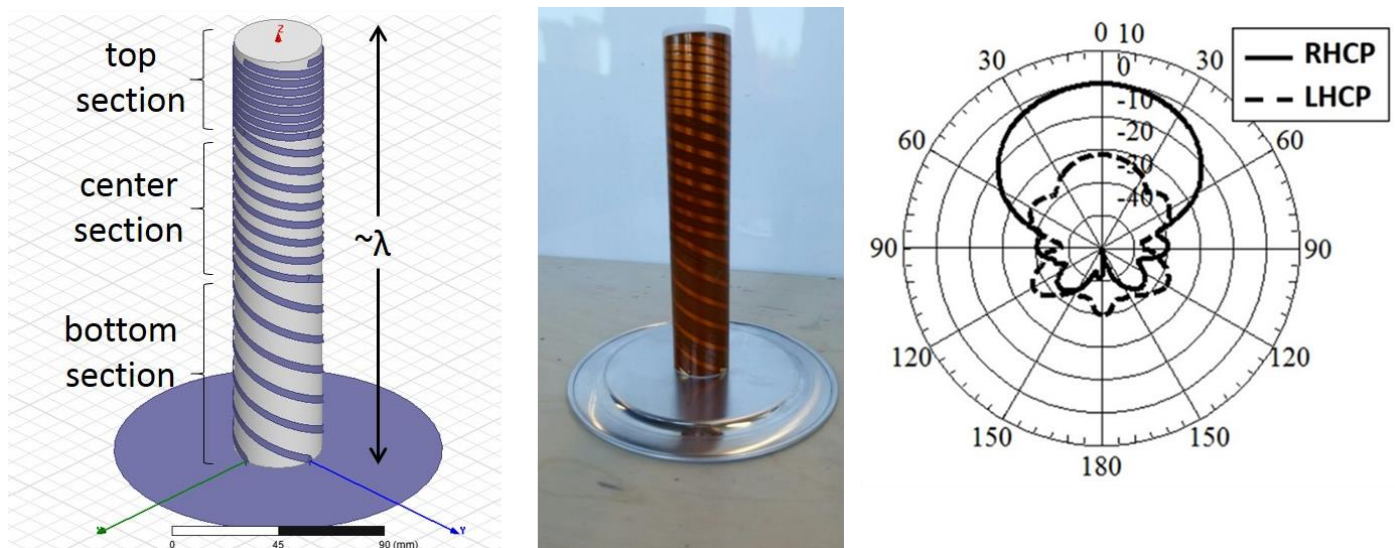


Figure 10. Simulation Model, Flexboard Prototype, and Measured Antenna Gain Pattern for the TSH Antenna.

Table 5. Important Parameters for the TSH.

Prototype Measurement Results: Three Stage Helix Antenna			
	Zenith RHCP Gain	RHCP Null Depth	LHCP Null Depth
Copper Tape Prototype	7.5 dBiC	30.9 dB	30.3 dB
Flexboard Prototype	0 dBiC	38.0 dB	37.3 dB

Figure 11 shows the prototype inductor helix antenna whose important gain parameters are given in Table 6. The IH has a 100-degree HPBW. The novel technical innovation was the use the surface mount inductors to phase the upper and lower helices to create the total horizon null.

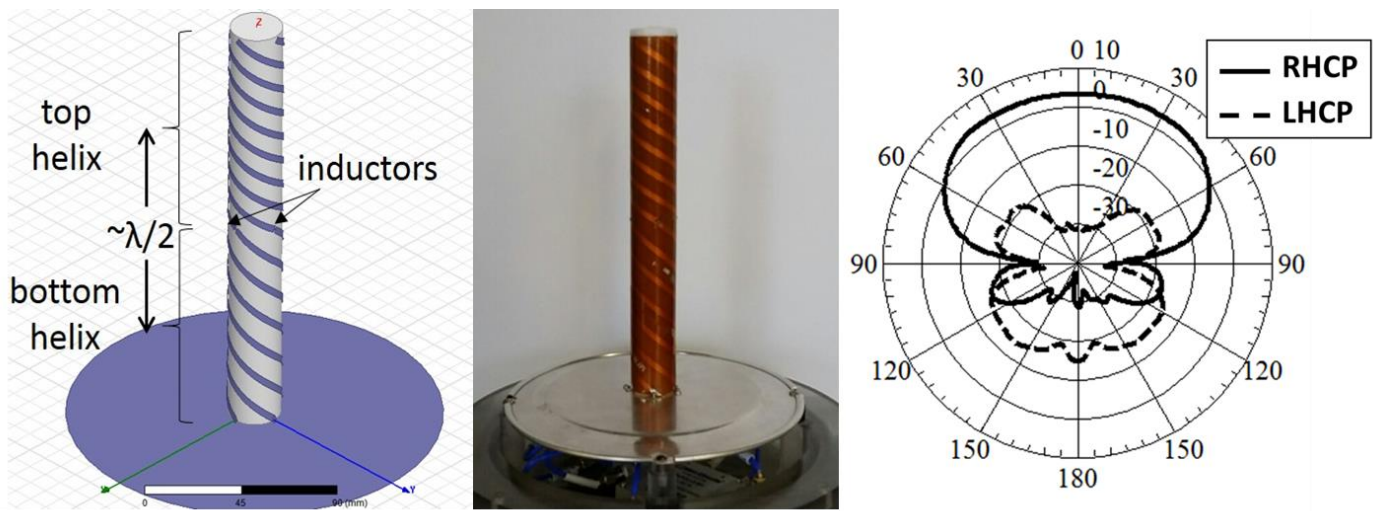


Figure 11. Simulation Model, Flexboard Prototype, and Measured Antenna Gain Pattern for the IH Antenna.

Table 6. Important Parameters for the IH.

Prototype Measurement Results: Inductor Helix Antenna			
	Zenith RHCP Gain	RHCP Null Depth	LHCP Null Depth
Copper Tape Prototype	4.0 dBiC	28.6 dB	34.4 dB
Flexboard Prototype	3.5 dBiC	30.2 dB	31.3 dB

The IH and TSH are similar in size, and the main physical difference between the IH and TSH is that the IH requires inductors to be soldered to the flexboard. Importantly, the IH has a substantially larger HPBW than the TSH.

The IH and TSH are plotted in Figure 2, which illustrates how they have substantially better combined horizon nulling at their given HPBW compared to the prototype and commercial antennas surveyed.

FIELD TEST RESULTS

The two prototypes were brought to a field test in 2016 where they were exposed to controlled jamming and spoofing signals. In addition to the prototype helix antennas, the prototype HRN antenna described in reference [9], a commercial timing antenna, and a commercial choke ring antenna were tested. The helix antennas provided up to 20 dB attenuation compared to the reference timing antenna (and 10-15 dB of attenuation compared to the choke ring). The HRN exhibited additional gain compared to the reference timing antenna due to its high LHCP gain at the horizon, which illustrated the importance of considering polarization in nulling antenna design.

The jamming attenuation of the antenna as measured in the field test is given in

Table 7 and compared against the “worst case predicted performance.” The prototype and choke ring antennas are compared to the reference timing antenna. The worst case predicted performance is the predicted interference attenuation for a jamming with polarization equal to the antenna’s highest horizon gain at any polarization, over all antenna azimuths. All antennas under test performed slightly worse than their worst case predicted performance indicating that the reference antenna could be outperforming predictions.

Table 7. Performance of Prototype Antennas at Field Test.

	Performance Relative to Reference Timing Antenna (dB)	
	Worst Case Predicted	Field Measurement
Timing	0	0
Choke Ring	13.39	5-10
Ring Nuller	14.3	-2 - 7
Three Section Helix	25	15-20
Inductor Helix	22.7	15-18

In addition to jamming signals, the antenna and the equipment connected to them were exposed to spoofing signals. The receivers connected to the helix antennas successfully operated through all spoofing environments whereas the receivers connected to the timing, choke ring, and ring nuller antenna all output position, velocity, and time information dictated by the spoofer.

FINDINGS AND CONCLUSIONS

The antenna survey found that there were no commercially available, or prototype, GNSS antennas designed to place nulls at all polarizations in the direction of the horizon, while maintaining sufficient satellite visibility to ensure GPS time as of 2016. A majority of the critical infrastructure timing receivers surveyed can provide time while using a single satellite and with a known antenna location indicating that narrower HPBW antennas are acceptable.

A simulation model was used to determine that a 60-degree HPBW is sufficient to ensure that five of six receivers from the survey will have access to at least two satellites 99 percent of the time installed on any major landmass or island. Two prototype helix antennas were built that met or exceed these specifications. Field tests of the prototype antennas demonstrated 15-20 dB of jammer suppression compared to a reference timing antenna. Receivers protected by the prototype antennas operated through a variety of spoofing scenarios that affected receivers connected to reference timing and choke ring antennas. Of the two prototype antennas, the inductor helix is preferred due to its larger HPBW.

ACKNOWLEDGEMENTS

The Homeland Security Act of 2002 (Section 305 of PL 107-296, as codified in 6 U.S.C. 185), herein referred to as the "Act," authorizes the Secretary of the Department of Homeland Security (DHS), acting through the Under Secretary for Science and Technology, to establish one or more federally funded research and development centers (FFRDCs) to provide independent analysis of homeland security issues. MITRE Corp. operates the Homeland Security Systems Engineering and Development Institute (HSSEDI) as an FFRDC for DHS under contract HSHQDC-14-D-00006. The HSSEDI FFRDC provides the government with the necessary systems engineering and development expertise to conduct complex acquisition planning and development; concept exploration, experimentation and evaluation; information technology, communications and cyber security processes, standards, methodologies and protocols; systems architecture and integration; quality and performance review, best practices and performance measures and metrics; and, independent test and evaluation activities. The HSSEDI FFRDC also works with and supports other federal, state, local, tribal, public and private sector organizations that make up the homeland security enterprise. The HSSEDI FFRDC's research is undertaken by mutual consent with DHS and is organized as a set of discrete tasks. This report presents the results of research and analysis conducted under:

HSHQDC-17-J-00100 Multi-GNSS Issues and Evaluation of PNT Mitigation Technologies

Sponsor: DHS Science & Technology First Responders Group

The purpose of this set of tasks is to (1) understand the implications of incorporating multi-GNSS (specifically foreign GNSS such as the European Galileo and Russian GLONASS) on critical infrastructure and (2) evaluate the effectiveness and performance of technologies that mitigate against PNT interference.

The results presented in this report do not necessarily reflect official DHS opinion or policy.

Approved for Public Release; Distribution Unlimited.

Case Number 18-0336 / DHS reference number 17-J-00100-03

REFERENCES

- [1] M. . Graham, "GPS Use in U.S. Critical Infrastructure and Communications," 23 10 2012. [Online]. Available: <https://www.gps.gov/multimedia/presentations/2012/10/USTTI/graham.pdf>. [Accessed 4 12 2017].

- [2] R. H. Mitch, R. C. Dougherty, M. L. Psiaki, S. P. Powell, B. W. O'Hanlon, J. A. Bhatti and T. E. Humphreys, "Signal Characteristics of Civil GPS Jammers," in *ION GNSS 2011*, Portland, Oregon, 2011.
- [3] T. E. Humphreys, B. M. Ledvina, M. L. Psiaki, B. W. O'Hanlon and P. M. Kintner, "Assessing the Spoofing Threat: Development of a Portable GPS Civilian Spoofer," in *Proceedings of the 21st International Technical Meeting of the Satellite Division of The Institute of Navigation (ION GNSS 2008)*, Savannah, GA, 2008.
- [4] J. Coffed, "The Threat of GPS Jamming," Exelis Inc, Rochester NY, 2014.
- [5] D. P. Shepard, T. E. Humphreys, , A. A. Fansler and , "Evaluation of the Vulnerability of Phasor Measurement Units to GPS Spoofing Attacks," *International Journal of Critical Infrastructure Protection*, vol. 5, 2012.
- [6] R. B. Rao, W. Kunysz, R. Fante and K. McDonald, *GPS/GNSS Antenna*, Artech House, 2012.
- [7] "Improving the Operation and Development of Global Positioning System (GPS) Equipment Used by Critical Infrastructure," [Online]. Available: [https://ics-cert.us-cert.gov/sites/default/files/documents/Improving_the_Operation_and_Development_of_Global_Positioning_System_\(GPS\)_Equipment_Used_by_Critical_Infrastructure_S508C.pdf](https://ics-cert.us-cert.gov/sites/default/files/documents/Improving_the_Operation_and_Development_of_Global_Positioning_System_(GPS)_Equipment_Used_by_Critical_Infrastructure_S508C.pdf). [Accessed 23 01 2018].
- [8] J. G. Geier, M. T. King and H. L. Kennedy, "Prediction of the time accuracy and integrity of GPS timing," in *IEEE Frequency and Control Symposium*, 1995.
- [9] I. T. McMichael, E. T. Lundberg, D. L. Hanna and F. S. Kolak, "A Horizon Ring Nulling Shorted Annular Patch Antenna with Shunted Stubs," *Progress In Electromagnetics Research M*, vol. 62, pp. 131-141, 2017.
- [10] "Free-space Path Loss," Wikipedia, [Online]. Available: https://en.wikipedia.org/wiki/Free-space_path_loss. [Accessed 25 01 2017].
- [11] J. W. Betz, *Engineering Satellite-Based Navigation and Timing*, Hoboken, New Jersey: Wiley, 2016.
- [12] "Evaluating the Minimum Antenna Half Power Beamwidth for Resilient GPS Time," 2017.
- [13] "IS-GPS-200H, GPS.GOV," 24 September 2013. [Online]. Available: <http://www.gps.gov/technical/icwg/>. [Accessed 25 January 2017].
- [14] C. A. Balanis, *Antenna Theory: Analysis and Design*, Hoboken: Wiley, 2005.
- [15] I. T. McMichael, E. T. Lundberg, D. Hanna and S. Best, "Horizon nulling helix antennas for GPS timing," in *2017 IEEE International Symposium on Antennas and Propagation & USNC/URSI National Radio Science Meeting*, San Diego, CA, 2017.